Cooling of a Gram-Scale Cantilever Flexure to 70 mK with a Servo-Modified Optical Spring

C. M. Mow-Lowry, A. J. Mullavey, S. Goßler,* M. B. Gray, and D. E. McClelland
The Centre for Gravitational Physics, Department of Physics, Faculty of Science, The Australian National University, ACT 0200, Australia
(Received 6 July 2007; published 8 January 2008)

A series of recent articles have presented results demonstrating optical cooling of macroscopic objects, highlighting the importance of this phenomenon for investigations of macroscopic quantum mechanics and its implications for thermal noise in gravitational wave detectors. In this Letter, we present a measurement of the off-resonance suspension thermal noise of a 1 g oscillator, and we show that it can be cooled to just 70 mK. The cooling is achieved by using a servo to impose a phase delay between oscillator motion and optical force. A model is developed to show how optical rigidity and optical cooling can be interchangeable using this technique.

DOI: 10.1103/PhysRevLett.100.010801 PACS numbers: 07.10.Cm, 04.80.Nn, 07.60.Ly, 42.50.Lc

A long term goal of experimental physics has been to reach the standard quantum limit or SQL [1,2] in the measurement of a mechanical oscillator. After the pioneering optical experiments of Tittonen *et al.* [3], the experiments closest to achieving this goal used nanomechanical electronic resonators [4,5]. In the optical domain, such experiments have uncovered significant new experimental physics, including a greater understanding of thermal noise, investigations of optical spring effects [6,7], and resonator cooling. Cooling can be broadly separated into "active," where the resonator is directly cooled via feedback [8–10], or "passive," where the cooling is achieved without servo-system feedback [11–14]. When optical cooling and optical rigidity are combined, it becomes feasible to cool a macroscopic object to the quantum ground state, revealing quantum effects for gram-scale objects [15,16]. In this Letter we present optical cooling in a hybrid regime where a servo system is used to alter the optical spring response.

The optical spring arises due to the nonzero gradient of the circulating power in a detuned Fabry-Perot resonator. The gradient of power to cavity length, and hence radiation pressure force to cavity length, determines the strength and sign of the optical spring. The magnitude of this effect is dependent on the input power P_{in}, the detuning from resonance (in increments of the cavity linewidth, or HWHM), δ, and the mirror properties. In the adiabatic limit—infinitely rapid response of the circulating power for a given length change—the optical spring "constant" is

$$k_0 = \frac{16\pi T_1 P_{\mathrm{in}}\sqrt{R_1R_2}\sin(\frac{\pi\delta}{\mathcal{F}})}{c\lambda[1 - 2\sqrt{R_1R_2}\cos(\frac{\pi\delta}{\mathcal{F}}) + R_1R_2]^2}, \qquad (1)$$

where R_1 and R_2 are the power reflectivities of the front and back mirror, respectively, T_1 is the power transmissivity of the front mirror, and $\mathcal{F}$ is the cavity finesse. Previous experiments have worked in this regime and have demonstrated the optical spring effect without observing cooling [6,17].

When the adiabatic condition is not valid, the magnitude and phase of the optical spring become a function of the frequency of motion. The phase of the optical spring, which is determined by the response time of the cavity, causes the optical spring to either damp or antidamp the resonant motion of an oscillator depending on the sign of the detuning [18]. For negative detunings, where the optical spring is an antirestoring force, the oscillator resonance is damped or cooled. For positive detunings, however, the cavity serves to enhance the resonant motion. This leads to optical heating, or, for sufficient antidamping, parametric instability [7,19,20]. This regime is of considerable importance for the planned upgrades to gravitational wave detectors, such as Advanced LIGO (Laser Interferometer Gravitational-Wave Observatory) [21], since any optical spring with a positive restoring force will also generate antidamping, potentially driving the detector away from its operating point as mechanical resonances are excited.

The optical spring may also be altered by a control system. A feedback loop changes the coupling between the motion of the oscillator, x, and the length change of the cavity, Δx, from 1:1 in the out of loop limit, to $\Delta x = x/(1 + G)$, where G is the complex loop gain. The optical spring then becomes (in the adiabatic limit)

$$k_g = \frac{k_0}{\sqrt{1 + 2G_0\cos(\psi) + G_0^2}} \qquad (2)$$

$$\theta_g = \tan^{-1}\left(\frac{-G_0\sin(\psi)}{1 + G_0\cos(\psi)}\right), \qquad (3)$$

where G_0 and ψ are the magnitude and phase of the loop gain. The terms k_g and θ_g are the magnitude and phase of the, now complex, optical spring. The angle θ_g determines whether the optical spring is purely real (a perfect spring), purely imaginary (a viscous damping force), or a combination of both.

The thermal noise of an oscillator with damping proportional to velocity (e.g., gas damping), is given by [22]

$$\hat{x}_{\rm th}^2 = \frac{4k_B T \phi \omega_0^2}{m\omega[(\omega^2 - \omega_0^2)^2 + (\phi\omega_0^2)^2]}, \tag{4}$$

where $\phi = \omega/(\omega_0 Q)$ is the mechanical loss angle, $\omega_0 = 2\pi f_0$ is the resonant frequency, m is the effective (modal) mass, and $T = 300$ K is the ambient temperature. When the effect of the optical spring is included, the modified thermal noise spectrum becomes

$$\hat{x}_{\rm th}^2 = \frac{4k_B T \phi \omega_0^2}{m\omega\{[\omega^2 - \omega_0^2 - k_g\cos(\theta_g)/m]^2 + [\phi\omega_0^2 + k_g \sin(\theta_g)/m]^2\}}. \tag{5}$$

From Eq. (5) it can be seen that there are two quadratures of the optical spring: one proportional to $\cos(\theta_g)$, which stiffens or weakens the mechanical spring, the other proportional to $\sin(\theta_g)$, which damps (cools) or antidamps (heats) the thermal peak. A similar model, which does not focus on the effect of the optical spring on thermal noise, is developed in [23].

In the case of active cooling, it is the servo system which directly suppresses thermal motion. In the passive case, it is the optical field which extracts the energy due to the response time of the optical oscillator. In the regime presented here, the loop gain is used to modify the optical field response. Thus the cooling is "passive" in the sense that it is the optical field which is extracting energy from our mechanical oscillator. A considerable advantage of this approach is that by altering the loop gain the optical spring may be shifted from pure rigidity ($\theta_g = 0$) to pure damping ($\theta_g = -90°$), as shown in Fig. 1 traces (a) and (b).

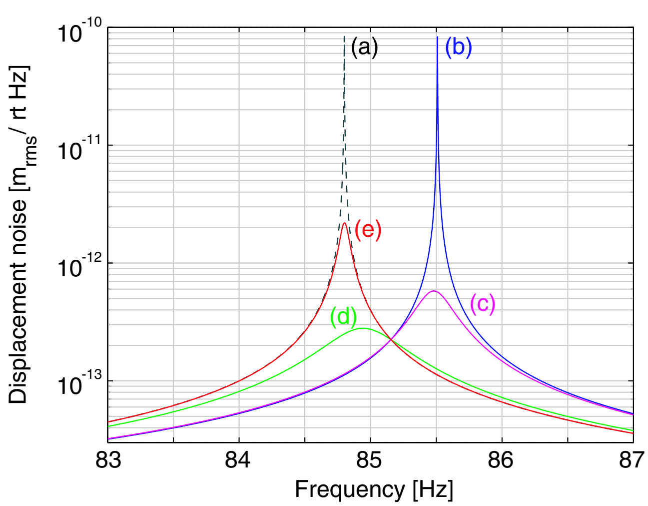

FIG. 1 (color online). Curve (a) shows the unmodified thermal noise. Curves (b)–(e) show how the optical spring is modified by loop gain—these traces have an input optical power of 1 mW, a detuning of $\delta = 0.5$, and the loop phase (ϕ) is $-90°$. Curve (b) shows pure optical rigidity (loop gain, $G_0 = 0$); curve (c) shows the onset of servo-induced optical cooling, where the servo begins imposing the $-90°$ loop phase onto the optical spring ($G_0 = 0.2$); curve (d) shows large optical damping ($G_0 = 2$); in curve (e), high servo gain suppresses the magnitude of the optical spring ($G_0 = 20$), which is now entirely in the damping quadrature.

Additionally, a small loop gain may be leveraged into a large cooling factor, as shown in Fig. 1 traces (c)–(e).

Our experiment measured the noise spectrum of a small, $L = 12.3$ mm, Fabry-Perot cavity—the "test cavity"—with a moveable output mirror and a finesse of 775. This small end mirror, 7 mm diameter, 1 mm thick, is glued to a y-shaped niobium beam which is monolithically attached via a cantilever flexure to a larger mounting block. This design was inspired by flexures contained in Ref. [24]. The flexure membrane is 72 μm thick, and the entire supported mass is of order 1 g. The effective (linearized) mass of this angular oscillator is 0.69 g, the fundamental resonance frequency is 84.8 Hz, and the quality factor is 44 500. A photograph of the flexure mounted mirror is depicted in Fig. 2 next to a schematic diagram of the experimental layout. The front mirror of the cavity is half an inch in diameter and is mounted on a piezoelectric transducer. Both mirror mounts are rigidly connected to a 2 kg stainless steel slab.

The test cavity is on a 2.5 m tall multistage vibration isolation system housed in a 5.5 m^3 vacuum tank. An optical breadboard 60 cm by 60 cm contains the final input beam steering optics. The test cavity is separately suspended on a single stage damped pendulum, designed to decouple the test cavity from the mechanical resonances of the in-vacuum steering optics and breadboard. With these measures, external seismic, acoustic, and mechanical vibrations all have a vastly attenuated effect beyond a measurement frequency of 5 Hz.

The laser is stabilized to a monolithic, Zerodur reference cavity of finesse 6000 which is mounted in a small vacuum chamber on a passively damped, single stage mechanical isolator.

The resonance condition of the test cavity was monitored using a ND:YAG laser and the Pound Drever Hall (PDH) technique [25]. This signal acted as both the principal readout and as the error signal for a servo system to lock the test cavity length to the laser frequency. The closed loop gain was measured *in situ* to ensure that the suppression of the signal by the control system was known and corrected for, and to determine the effect of the control system on the optical spring. The voltage spectrum was calibrated by determining the slope of the PDH error signal (in meters per volt) using an analytic model of the cavity frequency response, with the rf sidebands as frequency references. In addition, calibration lines were injected at

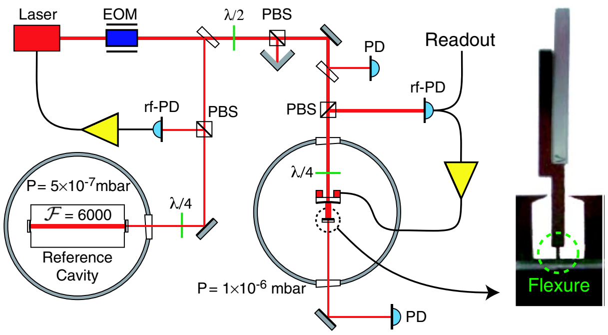

FIG. 2 (color online). A schematic diagram of the experiment. The triangles in the diagram encapsulate all servo-system electronics, i.e., demodulation, amplification, and filtering. Vacuum pressures are indicated next to the chambers. PBS = polarizing beam splitter, PD = photodetector, EOM = electro-optic modulator, and $\lambda/4$ = quarter wave plate. The photograph shows the flexure (circled) and mirror from the side.

33 Hz and 723 Hz (marked in Fig. 3) to correct for any change in the loop gain and error signal slope when the cavity was detuned from resonance. The servo has a simple $1/f$ integrator response resulting in a closed loop phase of $-90°$. The unity gain frequency of the loop was typically 500 Hz with a gain of around 6 at the 84.8 Hz resonance.

A variable offset was injected into the servo, detuning the zero-crossing point of the PDH signal away from the resonant peak of the cavity and introducing an optical spring. The reference trace in Fig. 3 shows that thermal noise, with no free variables in either the calibration or thermal noise model, is the dominant noise source in the region from 30 Hz to 200 Hz. The model for thermal noise used here assumes mechanical dissipation proportional to velocity. The mechanism for this damping is not well understood, but given the measured noise curve a thermal noise model assuming structural damping (with our measured Q) cannot fit our data. A fuller description of the experiment, model, and potential noise sources are given in Ref. [26].

The reference noise spectrum in Fig. 3 was influenced by the optical spring, despite efforts to minimize this effect. The strength of the antidamping was such that if the cavity drifted too close to the "unstable side" of resonance, it received a small kick to the end mirror, starting a runaway process. To prevent this instability, the cavity was slightly detuned from resonance to ensure the viscous optical damping remained positive. In order to reduce the magnitude of the optical spring to a level where the mechanical damping is always greater than the optical antidamping requires an input power of approximately 3 μW, an inoperably low power level for our experiment. This level of radiation pressure sensitivity meant that we were able to record traces with overwhelmingly large optical damping, resulting in very low effective temperatures.

The input optical power and detuning were both varied over a range of parameters. The input optical power was determined by continuously monitoring a calibrated portion of the input power. The detuning was determined by comparing the voltage offset injected into the test cavity locking servo with a model of the error signal (in Volts) versus detuning. The agreement between model and data is within 20%, and is confirmation of Eq. (5)—again, there are no fitted parameters. The "cooled" trace in Fig. 3 clearly shows that while the fundamental resonance peak is damped, the background thermal noise of that same

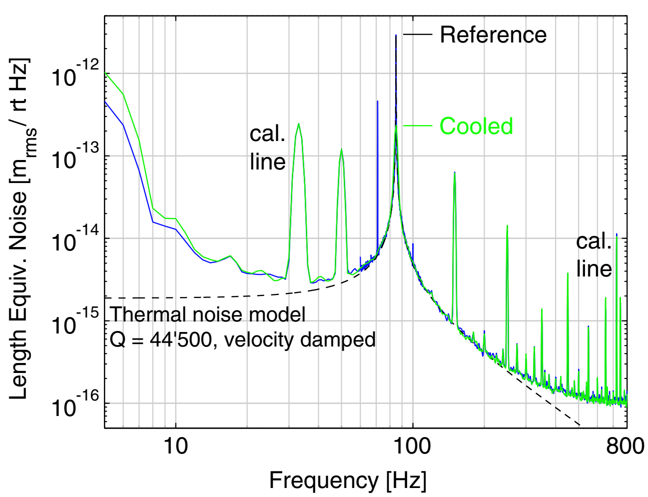

FIG. 3 (color online). Three traces are shown here: an experimental "reference" noise spectrum with the smallest operable detuning, showing that thermal noise is the dominant source of noise around resonance; a second noise spectrum showing that even with substantial optical cooling, the background noise remains unchanged—the peak height is at the same level as the marker, and the power and detuning are the same as in Fig. 4 trace (d); and finally, a thermal noise model.

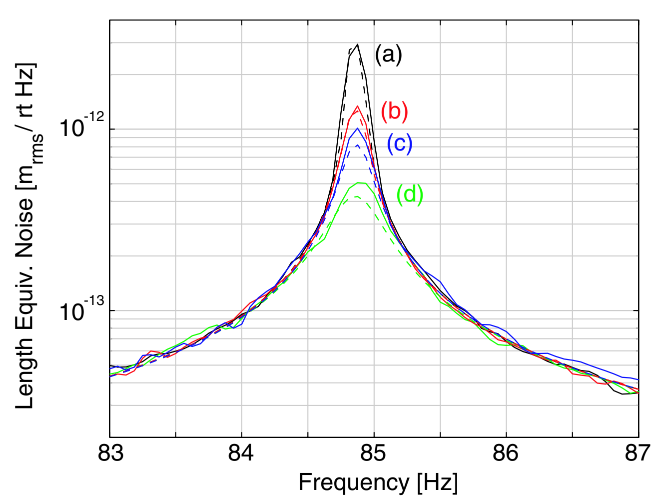

FIG. 4 (color online). A close zoom around the flexure-mirror mechanical resonance with an input power of 1.6 mW. As the cavity detuning increases from trace (a)–(d), so too does the optical damping. The dashed lines show the predicted peak height [from Eq. (5)] and the solid lines are experimental data.

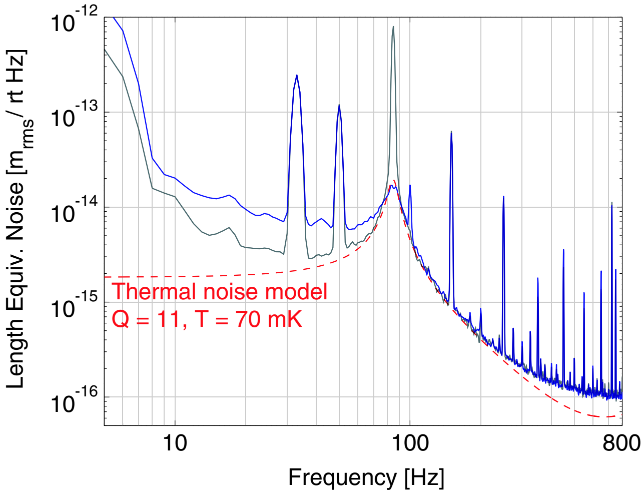

FIG. 5 (color online). High power (94 mW) and large detuning ($\delta = 0.25$) lead to extreme optical cooling. The pale gray trace is the same as the reference trace in Fig. 3.

mode does not increase. This means the optical spring is extracting thermal energy from the oscillator, or cooling it. Figure 4 demonstrates cooling of the mode as detuning increases, in agreement with our model. The effective temperature of the mode decreases in direct proportion to the increasing effective loss angle.

For higher powers and detunings there was an increase in noise below 85 Hz. This additional noise is thought to be classical intensity noise (perhaps caused by alignment-intensity coupling at the cavity) which couples in more strongly as the cavity is detuned, or possibly classical radiation pressure disturbing the flexure, again a coupling which causes larger noise for larger power and detuning.

This increase in low frequency noise does not skew the measurement of the effective temperature of the oscillator, since above resonance the noise is unaffected and still matches the thermal noise predictions. Figure 5 shows the most damped, or coldest, spectrum we recorded. The effective temperature was determined by substituting $\phi_{\rm eff}$ and $T_{\rm eff}$ for ϕ and T in Eq. (4), where $\phi_{\rm eff}$ is the combined optical and mechanical loss angle. The effective temperature is then found when $T_{\rm eff}$ is fitted such that the thermal noise model matches the data. In this way, we determined the coldest temperature of our gram-scale oscillator to be 70 mK, a cooling factor of 4300.

The results shown here are the first reported measurement of off-resonance suspension thermal noise in the LIGO detection band [27]. In addition, we showed that cooling of a thermal mode does not disturb the off-resonant noise of that mode, an assumption central to the association of an effective temperature with the mode [15]. The model developed shows the dependence of the thermal noise spectrum on optical rigidity and optical damping, and how the ratio of these can be altered using a servo system.

This research was completed under the auspices of ACIGA supported by the Australian Research Council.

*Current address: Max-Planck-Institut für Gravitationsphysik, Albert-Einstein-Institut, Callinstrasse 38, D-30167 Hannover, Germany.

[1] C. M. Caves *et al.*, Rev. Mod. Phys. **52**, 341 (1980).
[2] V. B. Braginsky, F. Y. Khalili, and K. S. Thorne, *Quantum Measurement* (Cambridge University Press, Cambridge, England, 1995).
[3] I. Tittonen *et al.*, Phys. Rev. A **59**, 1038 (1999).
[4] M. D. LaHaye *et al.*, Science **304**, 74 (2004).
[5] A. Naik *et al.*, Nature (London) **443**, 193 (2006).
[6] B. S. Sheard *et al.*, Phys. Rev. A **69**, 051801 (2004).
[7] T. Corbitt *et al.*, Phys. Rev. A **74**, 021802 (2006).
[8] P. F. Cohadon, A. Heidmann, and M. Pinard, Phys. Rev. Lett. **83**, 3174 (1999).
[9] D. Kleckner and D. Bouwmeester, Nature (London) **444**, 75 (2006).
[10] M. Poggio *et al.*, Phys. Rev. Lett. **99**, 017201 (2007).
[11] C. H. Metzger and K. Karrai, Nature (London) **432**, 1002 (2004).
[12] S. Gigan *et al.*, Nature (London) **444**, 67 (2006).
[13] O. Arcizet *et al.*, Nature (London) **444**, 71 (2006).
[14] J. G. E. Harris, B. M. Zwicki, and A. M. Jayich, Rev. Sci. Instrum. **78**, 013107 (2007).
[15] T. Corbitt *et al.*, Phys. Rev. Lett. **98**, 150802 (2007).
[16] T. Corbitt *et al.*, Phys. Rev. Lett. **99**, 160801 (2007).
[17] A. Dorsel *et al.*, Phys. Rev. Lett. **51**, 1550 (1983).
[18] V. B. Braginsky and S. P. Vyatchanin, Phys. Lett. A **293**, 228 (2002).
[19] V. B. Braginsky, S. E. Strigin, and S. P. Vyatchanin, Phys. Lett. A **287**, 331 (2001).
[20] C. Zhao *et al.*, Phys. Rev. Lett. **94**, 121102 (2005).
[21] http://www.ligo.caltech.edu/advLIGO/.
[22] P. R. Saulson, Phys. Rev. D **42**, 2437 (1990).
[23] S. W. Schediwy *et al.* (to be published).
[24] L. Ju, M. Baker, and D. G. Blair, Phys. Lett. A **280**, 182 (2001).
[25] R. W. P. Drever *et al.*, Appl. Phys. B **31**, 97 (1983).
[26] C. M. Mow-Lowry *et al.* (to be published).
[27] We note that off-resonance thermal noise was reported previously for lower Fourier frequencies in Appendix A of: C. D. Hoyle *et al.*, Phys. Rev. D **70**, 042004 (2004).